Published March 11, 2013

Journal of Environmental Quality TECHNICAL REPORTS

ORGANIC COMPOUNDS IN THE ENVIRONMENT

Evidence of Micropore Filling for Sorption of Nonpolar Organic Contaminants by Condensed Organic Matter

Yong Ran,* Yu Yang, Baoshan Xing, Joseph J. Pignatello, Seokjoo Kwon, Wei Su, and Li Zhou

Although microporosity and surface area of natural organic matter (NOM) are crucial for mechanistic evaluation of the sorption process for nonpolar organic contaminants (NOCs), they have been underestimated by the N_2 adsorption technique. We investigated the CO_2–derived internal hydrophobic microporosity (V_o) and specific surface area (SSA) obtained on dry samples and related them to sorption behaviors of NOCs in water for a wide range of condensed NOM samples. The V_o is obtained from the total CO_2–derived microporosity by subtracting out the contribution of the outer surfaces of minerals and NOM using N_2 adsorption–derived parameters. The correlation between V_o or CO_2–SSA and fractional organic carbon content (f_{OC}) is very significant, demonstrating that much of the microporosity is associated with internal NOM matrices. The average V_o and CO_2–SSA are, respectively, 75.1 μL g^{-1} organic carbon (OC) and 185 m^2 g^{-1} OC from the correlation analysis. The rigid aliphatic carbon significantly contributes to the microporosity of the Pahokee peat. A strong linear correlation is demonstrated between V_0/f_{OC} and the OC-normalized sorption capacity at the liquid or subcooled liquid–state water solubility calculated via the Freundlich equation for each of four NOCs (phenanthrene, naphthalene, 1,3,5-trichlorobenzene, and 1,2-dichlorobenzene). We concluded that micropore filling ("adsorption") contributes to NOC sorption by condensed NOM, but the exact contribution requires knowing the relationship between the dry-state, CO_2–determined microporosity and the wet-state, NOC-available microporosity of the organic matter. The findings offer new clues for explaining the nonideal sorption behaviors of NOCs.

Sorption and sequestration of nonpolar organic contaminants (NOCs) by natural organic matter (NOM) associated with aquifers, soils, and sediments control the bioavailability, risk, and fate of NOCs (Pignatello and Xing, 1996; Luthy et al., 1997; Brusseau et al., 1991). However, the physicochemical mechanisms of sorption/desorption and reduced bioavailability for NOCs remain unclear. Some investigators have recognized the importance of organic matter porosity and surface properties in controlling the magnitude and rates of sorption (Pignatello and Xing, 1996; Kleineidam et al., 2002; Nam and Alexander, 1998; Li and Werth, 2001; Ran et al., 2002, 2004).

The chemical, structural, and surface heterogeneity of NOM may strongly influence NOC sorption and desorption rates and equilibria in soils and sediments (Pignatello and Xing, 1996; Luthy et al., 1997; Ran et al., 2004). Natural organic matter has been characterized as comprising multiple domains or components, some of which can be characterized as partitioning phases and others as pore-filling phases (Xing and Pignatello, 1997; Weber and Huang, 1996; Ran et al., 2003). Depending on original source and diagenetic alteration histories, NOM in soils and sediments may be comprised of different types of organic materials, including biopolymer, humus, kerogen and coal materials, and black carbon from burning. Condensed organic matter, such as that which exists in humic substances, kerogen, and coal (Weber and Huang, 1996; Ran et al., 2003; Cornelissen et al., 2005), is generally recognized to behave like a glassy, polymer-like sorbent, whereas black carbon is generally recognized to be a nanoporous sorbent (Luthy et al., 1997; Allen-King et al., 2002). Condensed organic carbon phases could be major components of NOM in soils and sediments (Ran et al., 2002, 2007).

The microporosity and surface characteristics of NOM are crucial for the mechanistic evaluation of the sorption equilibrium and kinetics process. Steinberg et al. (1987)

J. Environ. Qual. 42:806–814 (2013)
doi:10.2134/jeq2012.0286
Supplemental data file is available online for this article.
Received 20 July 2012.
*Corresponding author (yran@gig.ac.cn).

Y. Ran and Y. Yang, State Key Lab. of Organic Geochemistry, Guangzhou Institute of Geochemistry, Chinese Academy of Sciences, Guangzhou 510640, Peoples' Republic of China; B. Xing, Dep. of Plant, Soil, and Insect Sciences, Univ. of Massachusetts, Amherst, MA 01003; J.J. Pignatello and Seokjoo Kwon, Dep. of Environmental Sciences, The Connecticut Agricultural Experiment Station, 123 Huntington St., P.O. Box 1106, New Haven, CT 06504-1106; W. Su and L. Zhou, School of Chemical Engineering, Tianjing Univ., Tianjing 300072, Peoples' Republic of China. Assigned to Associate Editor Ying Ouyang.

Abbreviations: DM, Dual-mode; DR, Dubinin-Radushkavich; Naph, naphthalene; NOC, nonpolar organic contaminant; NOM, natural organic matter; OC, organic carbon; Phen, phenanthrene; PP, Pahokee peat; SSA, specific surface area; TCB, 1,3,5-trichlorobenzene..

attributed the persistence of 1,2-dibromoethane in field soils to entrapment in "remote" intraparticle micropores. However, the contribution of NOM to soil and sediment microporosity has historically been considered negligible, principally because the surface area of NOM was estimated by the traditionally recommended N_2 adsorption technique (Xing and Pignatello, 1997; De Jonge and Mittelmeijer-Hazeleger, 1996; Ravikovitch et al., 2005; Kwon and Pignatello, 2005). Large discrepancies were reported between NOM surface areas derived from CO_2 adsorption and N_2 adsorption, primarily because of the activated diffusion and molecular sieving phenomenon (Xing and Pignatello, 1997; De Jonge and Mittelmeijer-Hazeleger, 1996). Activation diffusion and the molecular sieving effect in polymer network and hydrophobic microporous materials occur by a series of activated jumps along adsorption sites and are governed primarily by steric energy barriers (Gregg and Sing, 1982; Kärger and Ruthven, 1992). The adsorption/desorption steps require a finite activation energy derived from the temperature-dependent vibration amplitudes of an adsorbent and an adsorbate. When the experimental temperature is lower than a critical point, adsorbate molecules are unable to diffuse into the pores. In materials containing pores smaller than 0.5 nm, the surface area can be underestimated by BET-N_2 (Walker and Kini, 1965; Gan et al., 1972; Larsen et al., 1995). However, CO_2 is not affected by molecular sieving primarily because of the higher experimental temperature applied (usually 273K). Hence, CO_2–derived surface areas of coal and organic polymers were found to be one or two orders of magnitude higher than the N_2 surface areas (Xing and Pignatello, 1997; De Jonge and Mittelmeijer-Hazeleger, 1996). Moreover, it was observed that CO_2 yielded an approximately correct surface area for coals based on the agreement between CO_2 adsorption and small-angle X-ray scattering or small-angle neutron scattering techniques (Larsen et al., 1995). Also, ^{129}Xe NMR exchange spectroscopy supplied direct evidence for gas diffusion in different coal micropores (Zhu et al., 1997). However, there is no consensus on how important the microporosity and surface area in NOM and minerals are for the sorption of NOCs. How micropore volume and size distribution measured by CO_2 adsorption by dry samples are related to the aqueous sorption capacity for any of NOCs on the various NOM has not been systematically investigated.

In this study, we hypothesized that micropores in glassy NOM could serve as sorption domains for NOCs. We used a wide range of geosorbents, ranging from modern soils and sediments to diagenetically altered and physically condensed peat fractions, kerogen isolates, and coals, as sorbents and four NOCs as model sorbates, and the gas and aqueous adsorption data were used to test this hypothesis.

Materials and Methods

Samples

Two surface sediment samples (0–20 cm), MC37 and MC45, were collected from the Macao estuary of the Pearl River, China, using a box-sampling collector. Pahokee peat (PP) was purchased from the International Humic Substances Society. A portion of PP was treated with NaOH to extract the soluble humic substances, followed by HCl/HF to remove the mineral fraction, termed TP. Another portion of PP was demineralized with HCl/HF only and termed FP. The details of these treatments were given by Ran et al. (2002). Borden aquifer (BS-O) was collected from the Borden airforce base, Ontario, Canada, and a portion of the aquifer was treated with 1 mol L^{-1} HCl and called BS-T, and its kerogen isolates (BSK I and II) were separated with an HCl/HF acid demineralization procedure (Ran et al., 2003). Nonhydrolyzable organic matter (HP05) was obtained by treating soil collected near Guangzhou suburban area with trifluroacetic acid and hydrogen chloride; its properties are similar to kerogen (Ran et al., 2007). Beulah-Zap lignite was obtained from the American Argonne Premium coal bank. Three other raw coals, a subbituminous (JP) and two bituminous (XW and XA), were collected from nationally owned coal mines in China (Chen et al., 2005).

Nitrogen Gas and Carbon Dioxide Gas Adsorption

Surface analysis was performed as described previously (Xing and Pignatello, 1997; Kwon and Pignatello, 2005; Zhou et al., 2003). Samples were outgassed at 373K for 4 to 24 h. Low-pressure CO_2 isotherms were determined at 273K between 1×10^{-6} and 0.03 relative pressure on an Autosorb-1 (Quantachrome Instrument Corp.). From these isotherms we obtained pore size distribution and cumulative surface area up to 1.4 nm using Grand Canonical Monte Carlo simulation and density functional theory calculations using built-in software. For the high-pressure experiment, CO_2 adsorption isotherms at 273K and up to 3.46 MPa were performed in a DMT high-pressure microbalance (Sartorius 4406) (Zhou et al., 2003). The equilibrium time for each point takes about 10 h. The values were corrected for sample buoyancy effects and adsorption by the sample holder and pan. Sample buoyancy was estimated as the product of the skeletal volume of the sample and gas density. Nitrogen gas adsorption was performed at 77K using an ASAS 2010 volumetric gas analyzer (Micromeritics). The N_2–BET specific surface area (SSA) and total pore volume (V_t) were calculated from the Brunaur-Emmett-Teller method applied in the region of relative pressures from $p/p_o = 0.05$ to $p/p_o = 0.3$ and at relative pressure $p/p_o = 0.99$, respectively.

By attributing all the CO_2 adsorption to condensation in microvoids, one can calculate the microvoid volume ($V_{o,d}$) using the Dubinin-Radushkavich (DR) equation and Dual-mode (DM) equation:

$$\text{Log } V = \log V_{o,d} - D(\log p_o/p)^2 \quad [1]$$

$$V = K p/p_o + b\, Q_o\, p/p_o(1 + b\, p/p_o) \quad [2]$$

where V and $V_{o,d}$ are the adsorbed and micropore volumes (μL g^{-1}) expressed as a liquid volume (assuming the liquid density of CO_2 is 1.072 cm^3 g^{-1}), D is a constant related to the energy of adsorption and the pore structure, K is the partitioning coefficient for linear sorption, b is the parameter for the Langmiur equation, and Q_o is the adsorption parameter for the Langmiur equation. For the CO_2–SSA calculation, the cross-sectional area of CO_2 is 0.202 nm^2 calculated from its liquid density and molecular weight.

Sorption Isotherms

The sorption isotherms of phenanthrene (Phen) by the four coals, Borden kerogen fraction II, and nonhydrolyzable organic matter (HP05) were investigated in this study. The sorption isotherms of Phen, naphthalene (Naph), 1,3,5-trichlorobenzene (TCB), and 1,2-dichlorobenzene (DCB) by the two Borden sands and kerogen fraction I, three peat fractions, and two sediments were cited from our previous work (Ran et al., 2002, 2003). The physicochemical properties, such as octanol–water partition coefficients (log K_{ow}), aqueous solubilities (S_w), supercooled aqueous solubilities (S_{scl}), and the K_{oc} values (organic carbon–normalized sorption coefficient) are listed in Supplemental Table S1. Sorption equilibria were measured using completely mixed batch reactors consisting of flame-sealed glass ampules (50 mL; Kimble). Reactors were mixed continuously in a rotary shaker set at 125 rpm on a horizontal mode for 6 wk. Solute concentrations were analyzed with reverse-phase HPLC. Details of the experimental procedures used have been reported previously (Ran et al., 2002, 2004).

The sorption equilibrium isotherms were fitted using SYSTAT software (Version 8.0, SYSTAT Inc.) to the Freundlich model

$$\log q_e = \log K_F + n \log C_e \quad [3]$$

and the modified Freundlich equation

$$\log q_e = \log K'_F + n \log C_r \quad [4]$$

where q_e and C_e are the equilibrium solid-phase and aqueous-phase solute concentrations expressed as $\mu g\ g^{-1}$ and $\mu g\ L^{-1}$, respectively; K_F [in $(\mu g\ g^{-1})/(\mu g\ L^{-1})^n$] and n are the Freundlich capacity parameter and the isotherm nonlinearity factor, respectively; K'_F is the modified Freundlich isotherm capacity coefficient, and C_r is the dimensionless aqueous phase concentration.

For weakly polar and sparely soluble compounds, C_r is related to solute activity (a) in water phase referenced to their respective pure liquid or supercooled liquid (scl) state at a given temperature (Carmo et al., 2000). For NOCs that are liquid at the experimental temperature, C_r is the ratio of C_e to the aqueous-phase solubility S_w. For NOCs that are solid at the experimental temperature condition, C_r is the ratio of C_e to S_{scl}.

Results and Discussion

Sorbent Natural Organic Matter

The samples represent a wide range of NOM, including humus, kerogen, and coal materials. Relevant physicochemical properties are given in Table 1. The organic carbon (OC) contents range from 0.021% by weight for the Borden aquifer sediment to 73.2% for the XA coal (Table 1). The index of NOM maturity, as the huminite or vitrinite reflectance (R_o) (Ran et al., 2002), varies between 0.35 and 1.70% for the PP, Borden kerogen isolates, and coals. The O/C and H/C atomic ratios decrease as the maturation degree of organic matter increases.

Surface Area Probed with Nitrogen Gas Adsorption

Nitrogen adsorption isotherms at 77K on the investigated peats, coals, aquifer kerogen isolates, and sediment are type II (Fig. 1), characteristic of materials whose surface area is not dominated by micropores (Gregg and Sing, 1982), defined as pores <2 nm wide. The N_2–SSA ranges from 1.91 to 33.9 $m^2\ g^{-1}$ (Table 1). The N_2–SSA value tends to be high when the ash content of the sample is high. The N_2–SSA tends to be low for the samples high in OC, such as the PP fractions and coals, which is consistent with other investigations (Xing and Pignatello, 1997; De Jonge and Mittelmeijer-Hazeleger, 1996). Adsorption of N_2 at 77K is low because the external surface area of NOM is intrinsically low. In addition, coatings of humic substances may effectively block access of micropores to N_2 at 77K, as demonstrated for black carbon (Kwon and Pignatello, 2005). Moreover, the interior regions of NOM are not penetrable by N_2 within experimentally attainable equilibration times because of activated diffusion and molecular sieving effect and because of limited flexibility of interfacial macromolecules at the low

Table 1. Physicochemical properties for the samples.†‡

Samples	C	H	N	O	O/C	H/C	N_2–SSA	N_2-V_t	CO_2–SSA	$V_{o,d}$	V_o	V_o/f_{OC}	Ash	R_o
	%						$m^2\ g^{-1}$	$cm^3\ g^{-1}$	$m^2\ g^{-1}$	$\mu L\ g^{-1}$			%	
JP	68.55	4.35	3.85	14.91	0.16	0.76	4.91	0.010	169	70.7	69.3	101	8.10	0.52
XA	73.19	3.62	4.14	3.63	0.04	0.59	1.61	0.006	118	49.3	48.7	66.5	13.91	1.70
XW	48.68	3.17	3.19	6.34	0.10	0.78	6.92	0.019	68.7	28.7	26.3	54.0	38.10	1.12
BSK I	0.74	nd§	nd	nd	nd	nd	27.6	0.136	29.2	12.2	2.65	358	79.57	0.66–0.82
BSK II	5.56	0.34	1.30	nd	nd	nd	33.9	0.166	77.3	32.3	20.6	370	74.24	0.66–0.82
PP	47.97	5.18	3.71	26.91	0.42	1.30	2.22	0.010	98.9	41.3	40.5	84.4	16.23	0.35
TP	52.86	5.65	3.97	26.05	0.37	1.28	2.21	0.007	59.9	25.0	24.2	45.8	11.47	0.35
FP	52.93	5.51	3.71	28.94	0.41	1.25	1.72	0.007	93.9	39.2	38.6	72.9	8.91	0.35
MC37	1.70	0.80	0.25	nd	nd	nd	16.9	0.051	23.9	10.0	4.15	244	92.31	nd
HP05	52.30	3.72	0.56	16.70	0.24	0.85	6.45	0.017	133	55.7	55.0	105	20.5	nd
BZ	68.13	4.51	1.07	19.00	0.21	0.79	1.74	0.006	206	86.0	85.0	125	6.59	0.50
BS-O	0.021	nd	nd	nd	nd	nd	0.40	nd	nd	nd	nd	nd	nd	nd
MC45	1.23	0.56	0.19	nd	nd	nd	nd	nd	nd	nd	nd	nd	nd	nd

† f_{OC}, fraction of organic carbon in the sorbent; R_o, huminite or vitrinite reflectance; SSA, specific surface area; V_o, CO_2–derived internal hydrophobic microporosity; $V_{o,d}$, microvoid volume; V_t, total pore volume.

‡ The elemental compositions and reflectance (R_o %) were cited for the JP, XA, and XW coals from Chen et al. (2005), for BZ lignite (recalculating from CO_2 adsorption data) from Larsen et al. (1995) and Özdemir et al. (2005), and for the others from Ran et al. (2002, 2003).

§ Not determined.

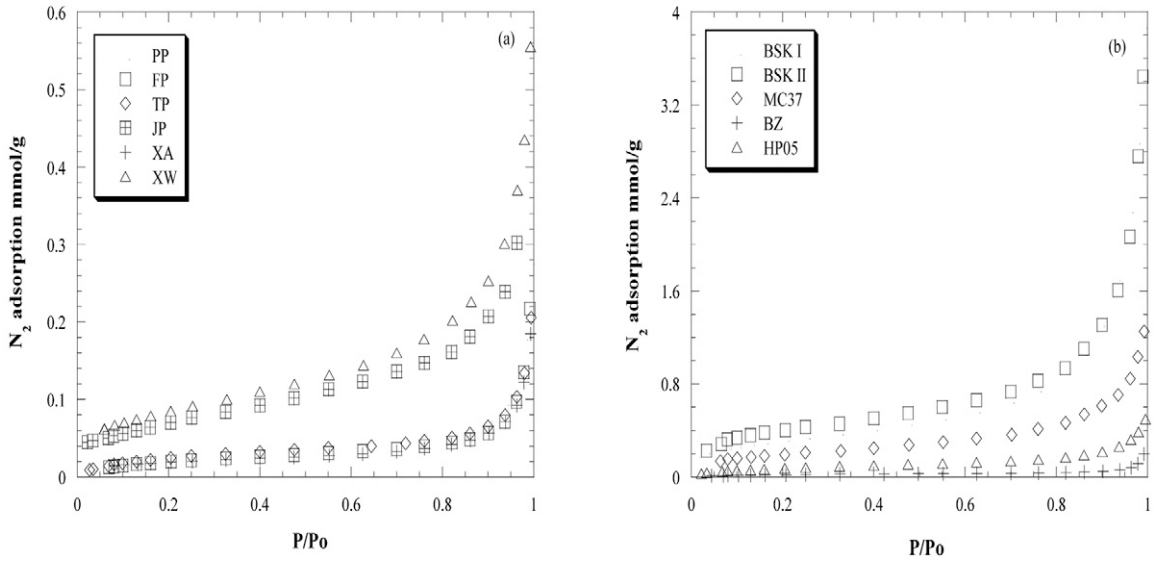

Fig. 1. Nitrogen gas adsorption isotherms on 11 the samples. (a) Three peat fractions (Pahokee peat [PP], PP demineralized with HCl/HF [FP], and PP treated with NaOH to extract the soluble humic substances followed by HCl/HF to remove the mineral fraction [TP]), and three coals (JP, XA, and XW). (b) Two Borden aquifer kerogen isolates (BSK I and II), one surface sediment (MC37), one coal (BZ), and nonhydrolyzable natural organic matter (HP05).

temperature of N_2 adsorption measurements (77K) (Pignatello et al., 2006). Thus, the surface areas obtained from N_2 are the ones contributed mainly by any exposed surface of the NOM/mineral soil particles.

Microporosity Probed with Carbon Dioxide Gas Adsorption

Carbon dioxide adsorption at 273K is one to two orders of magnitude greater than N_2 adsorption for the sorbents with high OC content (coals, peat fractions, and HP05) but is only about 1 to 3 times greater than N_2 adsorption for the other sorbents with low OC content (BSK I, BSK II, and MC 37) (Fig. 2). The CO_2 adsorption isotherms for the solids with moderate to high OC contents are nonlinear and well fitted to the Freundlich model [$W = K\,(p/p_o)^n$]. For BSK I, BSK II, and MC37, which have high ash contents and low OC contents, the CO_2 adsorption isotherms approach linearity.

The DR equation is well fitted to any of the low-pressure CO_2 adsorption isotherms ($p/p_o < 0.031$) or to data of the high pressure isotherms below $p/p_o = 0.3$ ($R^2 > 0.99$) (Fig. 2), and the calculated micropore volumes ($V_{o,d}$) are presented in Table 1. The micropore volume ranges from 10.0 to 86.0 μL g^{-1}. The $V_{o,d}$ value estimated from the high pressure CO_2 adsorption on PP in this study is the same as that reported for PP using the low pressure CO_2 adsorption (Xing and Pignatello, 1997). The CO_2–SSA ranges from 30 to 206 m^2 g^{-1}. The CO_2–SSA values

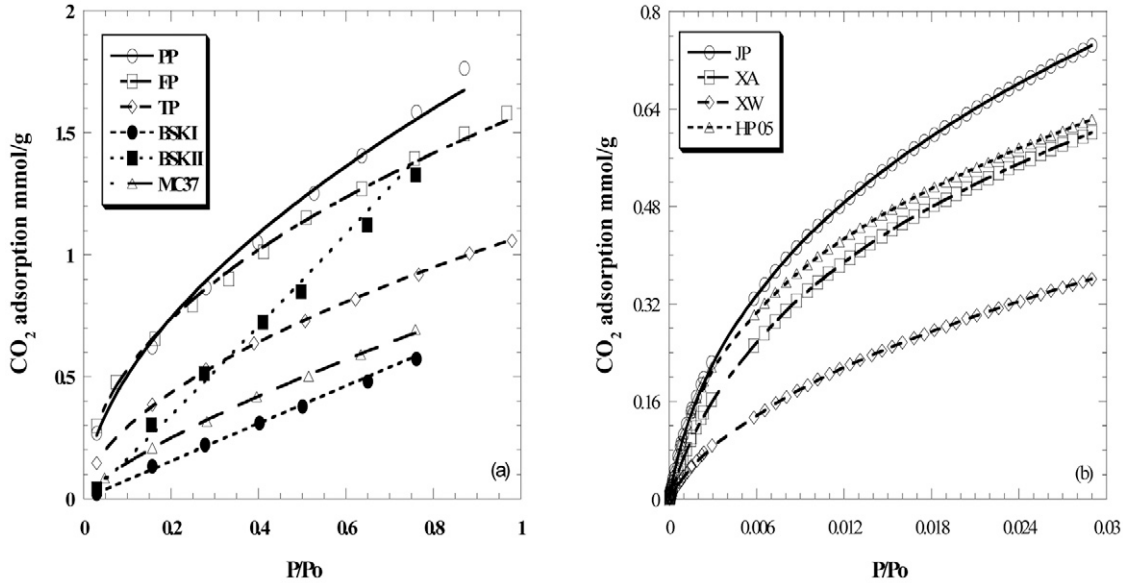

Fig. 2. Carbon dioxide adsorption isotherms on three peat fractions (Pahokee peat [PP], PP demineralized with HCl/HF [FP], and PP treated with NaOH to extract the soluble humic substances followed by HCl/HF to remove the mineral fraction [TP]), two Borden aquifer kerogen isolates (BSK I and II), one surface sediment (MC37), nonhydrolyzable natural organic matter (HP05), and three coals (JP, XA, and XW). (a) High-pressure CO_2 adsorption fitted to the Freundlich equation. (b) Low-pressure CO_2 adsorption fitted to the Dubinin-Radushkevitch equation.

for the four coals (85–206 $m^2\ g^{-1}$) obtained in this study are in the range of those measured using CO_2 at 295K for the eight American Argonne Premium coals (113–225 $m^2\ g^{-1}$) (Larsen et al., 1995; Ozdemir et al., 2005). The CO_2–SSA and micropore volume for the JP lignite are similar to those of the Beulah-Zap lignite (Table 1). As indicated above, the CO_2 adsorption data also include a contribution from the mineral surface. To correct for this contribution, we estimated the hydrophobic micropore volume (V_o) in Table 1 by using the difference between CO_2–SSA and N_2–SSA as well as the CO_2 molecular redius (r = 0.253 nm) [$V_o = (4r/3)(CO_2\text{–SSA} - N_2\text{–SSA})$].

Compared with N_2, CO_2 more strongly interacts with polar regions of NOM due to its quadrupolar moment. We must consider, therefore, whether CO_2 sorption to NOM is complicated by partitioning and swelling. The DM-derived Q_o values are smaller than the DR-derived $Q_{0,d}$ values in the majority of cases but are larger in other cases (Supplemental Table S3). Although the DM model often overestimates linear partitioning in NOM samples (Milewska-Duda et al., 2000; Ran et al., 2004), it is nevertheless difficult to compare parameters of different models when they are derived from different assumptions and theoretical perspectives. Low-pressure CO_2 adsorption shows low hysteresis for the three coals and HP05, whereas high-pressure CO_2 adsorption shows significant hysteresis for PP and TP (Supplemental Fig. S1). Such results suggest that matrix expansion of NOM is insignificant at low pressures but may be significant at higher pressures. In any event, previous studies of model and natural substances show that partitioning and swelling are unimportant for CO_2.

Some investigations found that expansion of coals by low-pressure CO_2 does not change micropore volume (Walker et al., 1988). Reucroft and Sethuraman (1987) measured the swelling of various ranks of Kentucky coal due to the adsorption of gases by directly observing directional (length) changes at pressures between 0 and 1.5 MPa. The volume increase observed in going from 0 to 1.5 MPa was between 0.36 and 4.18%. Walker et al. (1988) measured the expansion of powdered coals and macerals induced by gaseous CO_2 and concluded that the expansion is quite small at low pressure adsorption and that CO_2 uptake was primarily in micropores at the tested temperatures and pressures. Kwon and Pignatello (2005) showed that glass beads (1.7 g) coated with vegetable oil at the level of 5 or 14 wt % did not show increased CO_2 uptake compared with glass beads alone, thereby giving no evidence of CO_2 dissolution. Lattao et al. (2012) examined a 1:1 polymer blend of polystyrene and polyvinyl methyl ether, which contains both nonpolar aromatic and polar aliphatic groups and forms a homogeneous rubbery film when cast from toluene. That material sorbed little CO_2 (8.2 $\mu L\ g^{-1}$ OC) and showed negligible microporosity. Advanced analysis techniques, such as small-angle X-ray scattering and ^{129}Xe NMR, also supplied direct evidence for the dominance of microporosity in coals measured by CO_2 adsorption (Larsen et al., 1995; Zhu et al., 1997). We conclude, therefore, that the CO_2 adsorption isotherms on the NOM samples in this study demonstrate microporosity.

The pore size distribution profiles estimated from the CO_2 isotherm at 273K for the coals are presented in Supplemental Fig. S2. The pore size distribution indicates that micropores <0.7 nm account for about 58 to 73% of cumulative pore volume ranging from 0 to 1.4 nm. The cumulative pore volumes are 56.2, 45.3, and 31.5 $\mu L\ g^{-1}$ for JP, XA, XW coals, respectively.

Correlation between Gas Adsoprtion Parameters and Sorbent Properties

Figures 3a and 3b show that V_o and CO_2–SSA correlate linearly with OC content (R^2 = 0.72 and 0.73, respectively; p < 0.01). We found that the linear correlation for our samples agrees very closely with that obtained for pooled data from this study and from other investigations (Li and Werth, 2001; Xing and Pignatello, 1997; De Jonge and Mittelmeijer-Hazeleger, 1996) (Fig. 3). The slopes of the respective linear regression lines in Fig. 3 give an average micropore volume of 75.1 $\mu L\ g^{-1}$ OC and an average CO_2–SSA of 185 $m^2\ g^{-1}$ OC for condensed NOM, which is represented by a wide range of NOM type and maturation. Moreover, Fig. 3c shows that the N_2 SSA increases as the ash content increases and the OC content decreases. This means that N_2 and CO_2 probe different regions of the geosorbent matrix: N_2 primarily probes the outer surface of particles (NOM or mineral), whereas CO_2 additionally probes the internal porosity of NOM.

The correlation coefficients between CO_2–SSA or micropore volume and the total OC content in Fig. 3 account for about 72 to 73% of the variations for the investigated samples, suggesting that other factors, such as chemical compositions, structure, configuration, geochemical alteration of NOM, affect the microporosity and surface area. The reduced, diagenetically altered kerogen isolates and coals are generally rich in the microporosity. The BSK II fraction and lignite coals JP and BZ have considerably higher micropore volumes than the correlation line predicted. One exception is XW, which has lower microporosity than predicted. This might be related to its high ash content because minerals coated with NOM block and reduce its microporosity. As the maturation degree of coals increases from JP to XW and to XA (i.e., as R_o increases) (Table 1), the micropore volume decreases. This observation is consistent with other investigations. For example, Ozdemir et al. (2005) found that the micropore volume and surface area decrease as the rank of the eight Argonne Premium coals increases. For the four humic acid samples, two are lower than and the other two are close or higher than the correlation lines (Fig. 3a, b). Depending on their aliphatic and aromatic carbon concentrations and on oxygen-containing functional groups, they might have higher or lower microporosity than other types of condensed and glassy NOM (coal and kerogen).

The ^{13}C NMR spectrum for the nonhydrolyzable NOM HP05 exhibits two major peaks: one aliphatic carbon peak and one aromatic carbon peak (Ran et al., 2007). Its micropore volume is close to that of PP (Table 1; Fig. 3). For the three peat fractions, the ^{13}C NMR spectra measured indicate that TP and FP were altered due to base and/or acid treatment (Ran et al., 2002). Detailed analysis indicates that, in comparison with the original peat sample PP, TP has slightly higher OC and O-alkyl carbon content but lower content of aliphatic and methoxyl carbon (Supplemental Fig. S3), suggesting that aliphatic carbon (especially rigid all-trans region at 32.9 ppm) (Mao et al., 2001) and possibly lignin were partially removed and/or altered due to base and acid hydrolysis reactions induced by the

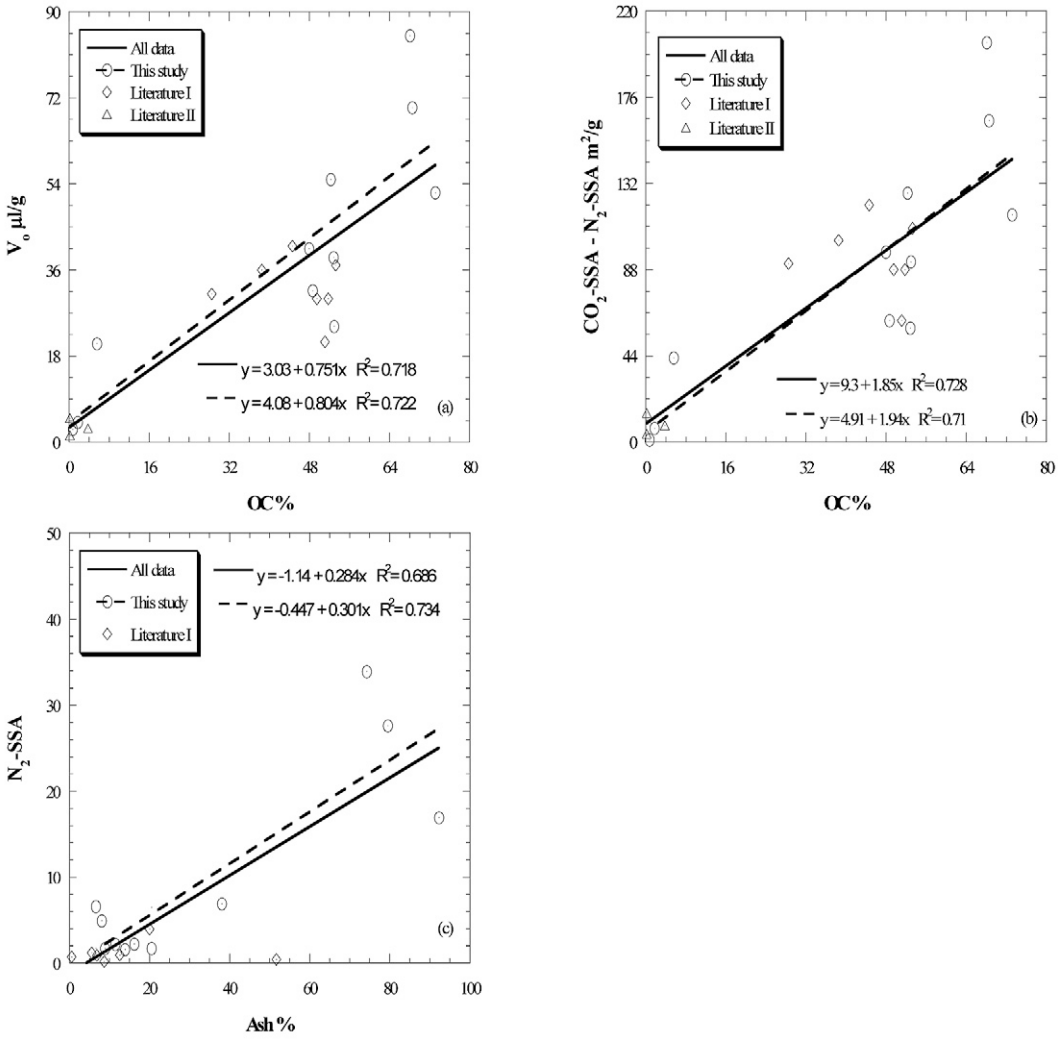

Fig. 3. Correlation of CO_2–derived internal hydrophobic microporosity (V_o), CO_2–specific surface area (SSA), and N_2–SSA with organic carbon (OC)% and Ash% in this study; in Literature I (Xing and Pignatello, 1997; De Jonge and Mittelmeijer-Hazeleger, 1996) for three peats, three humic acids, and one soil; and in Literature II (Li and Werth, 2001) for two aquifers and a soil. (a) V_o, (b) CO_2–SSA, and (c) N_2–SSA

treatments. During the 1 mol L^{-1} NaOH alkaline treatment, PP expanded sharply. Accordingly, micropore volume decreased in comparison with that of PP, suggesting that the rigid aliphatic carbon significantly contributes to the microporosity of NOM. However, the NOM structure of FP was not significantly changed during the demineralization treatment, and its micropore volume is similar to that of PP (Table 1). Moreover, previous investigations indicate that PP contains a very low concentration of black carbon, which accounts for only 1.5% of total OC (Ran et al., 2002) and does not preferentially sorb either of two NMR spin probe compounds according to analysis of the ^{13}C-CP/TOS-NMR spectra (Lattao et al., 2012). It was recently found that the aliphatic carbon of the type I kerogen contained considerable glassy carbon (Zhang et al., 2007). Hence, the microporosity for the peat factions originates from kerogen macerals and humic substances rather than from black carbon. The detailed relationship between the microporosity and the structure of NOM is discussed elsewhere (Sun et al., unpublished observations).

Correlation between Microporosity and Sorption Capacities of Nonpolar Organic Contaminants

The Phen sorption data in this study and those of Phen, Naph, TCB, and DCB in previous investigations (Ran et al., 2002, 2003) are used to investigate the correspondence between gas-phase and aqueous-phase sorption behaviors by NOM. The Freundlich log K_F and n parameter values, along with their standard deviations, number of observations, and R^2 values, are given in Table 2 for the investigated Phen sorption isotherms and in Supplemental Table S3 for the published sorption isotherms for Phen, Naph, TCB, and DCB. The data presented in Tables 2 and S3 and Supplemental Fig. S5 for the tested sorbent–sorbate systems show that the majority of the sorption isotherms for Phen, Naph, DCB, and TCB are nonlinear and can be quantified using the Freundlich model. The n values, which reflect the degree of linearity, are within the range of 0.64 to 0.85 for Phen and 0.79 to 0.90 for Naph, whereas the n values for TCB and DCB are 0.81 to 1.04 and 0.90 to 1.10, respectively. Based on the modified Freundlich sorption parameters in Tables 2 and S3, the sorption volume ($Q_{o,f}$) for each sorbent is calculated at the reduced concentration C_r levels of 0.05, 0.5, and 1 based

on S_w (for the liquid DCB) or S_{scl} (for the other compounds) and by using the density of each solute at the temperature of the isotherm. Basing $Q_{o,f}$ on C_r normalizes for chemical potential among all compounds at each concentration level.

Figures 4a, 4b, and 4c show a strong linear relationship between V_o and $Q_{o,f}$ at all three C_r levels and for each compound. Figure 4d and Supplemental Fig. S5a, S5b, and S5c show a strong linear correlation for each compound between the OC-normalized maximum sorption capacity ($Q_{o,f}/f_{OC}$ at C_r = 1) and OC-normalized hydrophobic micropore volume (V_o/f_{OC}), where f_{OC} is the fraction of OC in the sorbent (R^2 = 0.995, 0.794, 0.972, and 0.996 for Phen, Naph, TCB, and DCB, respectively). This result is consistent with the organic matter component as the source of the interaction. In each panel of Fig. 4, all compounds seem to fall on a common curve, suggesting that hydrophobic micropore filling is relatively insensitive to molecular size in the range represented by these test compounds. At maximum capacity (C_r = 1; Fig. 4c, d), a nearly perfect correlation (close to 1:1) exists between V_o and $Q_{o,f}$. At first glance, this result suggests that all or nearly all sorption of the NOCs by these sorbents is due to micropore filling. However, we do not know the relationship between the CO_2–determined V_o and the equivalent microporosity available to the NOCs. Carbon dioxide has access to more pores than the NOCs due to its smaller size. Moreover, the sorbent is likely to have been affected by being submerged in water. Water at high concentrations causes swelling and plasticization of NOM (Belliveau et al., 2000; Schaumann 2006a, b; Schaumann and LeBoeuf 2005; Schaumann et al., 2005), which could result in collapse of some micropores that otherwise exist in the dry state as a consequence of outgassing before CO_2 isotherm construction. Molecular size and hydration state correspond to the lower effective value of hydrophobic micropore volume for the NOCs compared with V_o. Nevertheless, the results indicate that microporosity contributes to the adsorption of NOCs in natural organic matter. If partitioning were the sole mode of sorption, then the correlation between $Q_{o,f}/f_{OC}$ and V_o/f_{OC} would likely be nonexistant.

The above evidence confirms our previous conclusion by using the combined linear partitioning–Polanyi adsorption modeling analysis (Ran et al., 2002, 2004). Furthermore, the estimation of the microporosity (75.1 μL g^{-1} OC) and SSA (185 m^2 g^{-1} OC) for the 21 samples (Fig. 3) is much higher than previously reported. Kleineidam et al. (2002) used the N_2 gas adsorption technique and reported mesopore and micropore volumes of 7.9 to 11.4 μL g^{-1} for the three Germany coals, with OC ranging from 38.9 to 72.1%. However, the range in V_o/f_{OC} is quite large (45.8–370 μL g^{-1} OC), with the largest values corresponding to the samples with low f_{OC} (BSK I, BSK II, and MC37). The micropore volumes may be much higher than the estimation value by the V_o–f_{OC} correlation in Fig. 3. If the relationship exhibited in Fig. 4d is correct, the micropore volume can reach 358 to 370 μL g^{-1} OC for two kerogen isolates from the Borden sand. The detailed relationship between the microporosity and the structure of NOM is discussed elsewhere (Sun et al., unpublished observations).

Environmental Implications

The nonlinear sorption of NOCs has been attributed to the compositional and structural heterogeneity of NOM (Xing and Pignatello, 1997; Weber and Huang, 1996; Pignatello, 2012). Surface and geometric heterogeneity, including pore size and shape, pore volume, and pore surface chemistry, are critical for adsorption of NOCs on activated carbon materials. Dubinin (1960) and Crittenden et al. (1999) reported that adsorption capacity and the exponent term for the Dubinin-Astakhov equation, which is similar to Eq. [1], were related only to the nature of the adsorbent. For an activated carbon and a synthetic glassy polymer, the adsorption volume of a given NOC can be close to or approximately half the experimental total micropore volumes, respectively (Crittenden et al., 1999).

The results described provide important implications for the interpretation of sorption mechanisms of organic contaminants in SOM. Our data support the concept of "adsorption" of NOCs in the internal micropores of NOM. Quantitative estimates of pore size and surface area derived from CO_2 adsorption allow for a more specific formulation of this concept. The majority of total surface area is formed by subnanometer scale pores.

Conclusions

We investigated the N_2 and CO_2–derived V_o and SSA and related them to sorption behaviors of NOCs in condensed NOM ranging from modern soils and sediments to diagenetically altered and physically condensed peat fractions, kerogen isolates, and coals. Carbon dioxide adsorption at 273K is one to two orders of magnitude greater than N_2 adsorption for the sorbents

Table 2. Freundlich sorption parameters and sorption capacities for phenanthrene.

Samples	log K_F†	n	R^2	Number of observations	$Q_{o,f}$‡		
					0.05 S_{scl}	0.5 S_{scl}	1.0 S_{scl}
					μL g^{-1}		
JP	2.14 ± 0.05§	0.71 ± 0.03¶	0.99	22	6.68	34.3	56.0
XA	1.46 ± 0.11	0.87 ± 0.05	0.98	18	3.51	26.0	47.5
XW	1.81 ± 0.08	0.64 ± 0.04	0.99	20	2.07	8.98	14.0
BZ	2.10 ± 0.10	0.75 ± 0.05	0.99	20	7.94	45.1	76.0
BSK II	1.57 ± 0.02	0.74 ± 0.02	1.00	24	2.11	11.5	19.2
HP05	1.61 ± 0.13	0.84 ± 0.07	0.98	18	4.18	28.8	51.6

† Unit in (μg g^{-1})/(μg L^{-1})^n.

‡ Sorption volume derived from sorption capacities using solute density. S_{scl}, supercooled aqueous solubilities.

§ Standard deviation of log K_F.

¶ Standard deviation of n.

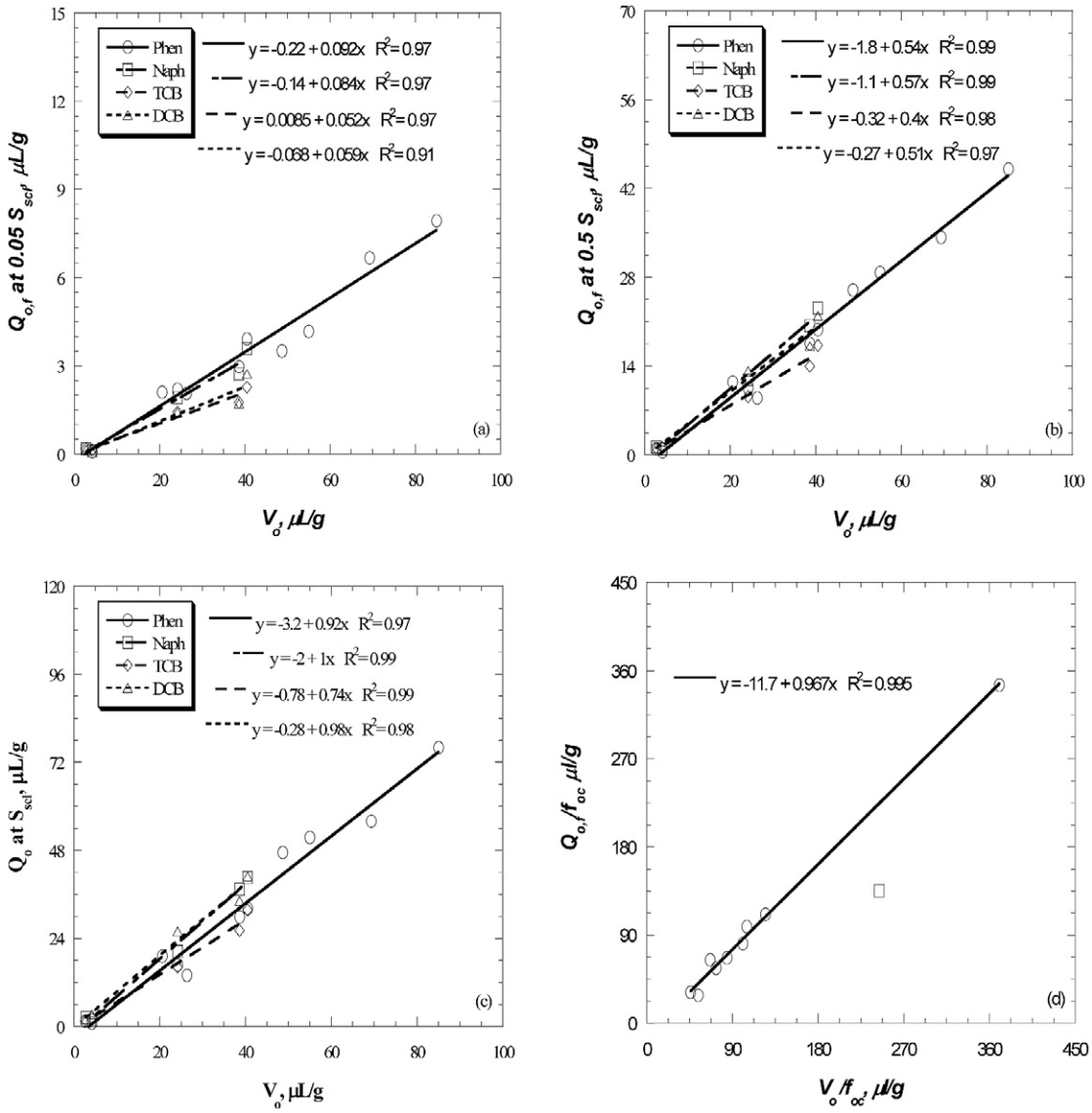

Fig. 4. Correlation between the sorption volume of phenanthrene (Phen) at each of three supercooled solubilities (S_{scl}) and CO_2–derived internal hydrophobic microporosity (V_o) on the 11 samples and between that of naphthalene (Naph), 1,3,5-trichlorobenzene (TCB), or 1,2-dichlorobenzene (DCB) and V_o on the five samples in Table 1. (a) Solute concentration is at 0.05 S_{scl}. (b) Solute concentration is at 0.5 S_{scl}. (c) Solute concentration is at S_{scl}. (d) Organic carbon–normalized case corresponding to panel c. MC-37 shown as a square mark is not included in the correlation.

with high organic matter concentrations but is about one to three times higher than N_2 adsorption for the other sorbents with low organic matter concentrations. Nitrogen gas primarily probes the outer surface of particles, whereas CO_2 additionally probes the internal porosity of NOM. The correlation between V_o or SSA and OC content (OC %) is significant, demonstrating that microporosity primarily originates from the NOM matrices. The average V_o and CO_2–SSA are 75.1 µL g^{-1} OC and 185 m^2 g^{-1} OC, respectively, from the correlation analysis. The rigid aliphatic carbon in the PP significantly contributes to the microporosity of NOM. A linear correlation is demonstrated between the hydrophobic micropore volume of the organic matter fraction and the sorption capacity of the organic matter fraction for each of four NOCs on an OC basis. The hydrophobic micropore volume is high enough to account for a sizable fraction of the sorption of NOCs, but the exact contribution depends on the relationship between the CO_2, dry-state microporosity and the NOC, wet-state microporosity of the NOM, which is yet to be determined.

Supplemental Material

Three tables listing selective physicochemical properties of the four sorbates, micropore volumes derived from various equations for CO_2 and Phen, and Freundlich sorption parameters for the three NOCs; five figures showing the sorption and desorption isotherms, the micropore size distribution, ^{13}C NMR spectra for the peat fractions, the sorption isotherms of Phen, and correlation between V_{OC}/f_{OC} and the Q_o/f_{OC} for Naph, TCB, or DCB.

Acknowledgments

The authors thank Dr. Yingjun Chen for providing the Chinese coals. This study was supported by a key project of NNSFC-Guangdong (U1201235), a key field project of Chinese Academy of Sciences (Y234081A07), a general project and a "Team Project" of National Natural Science Foundation of China (41073082 and 41121063),

and by the National Science Foundation of the United States (BES-0122761). This is contribution no. IS-1605 from GIGCAS.

References

Allen-King, R.M., P. Grathwohl, and W.P. Ball. 2002. New modeling paradigms for the sorption of hydrophobic organic chemicals to heterogeneous carbonaceous matter in soils, sediments, and rocks. Adv. Water Resour. 25:985–1016. doi:10.1016/S0309-1708(02)00045-3

Belliveau, S., T. Henselwood, and C. Langford. 2000. Soil wetting processes studied by magnetic resonance imaging: Correlated study of contaminant uptake. Environ. Sci. Technol. 34:2439–2445. doi:10.1021/es990299p

Brusseau, M.L., R.E. Jessup, and P.S.C. Rao. 1991. Nonequilibrium sorption of organic chemicals: Elucidation of rate-limiting processes. Environ. Sci. Technol. 25:134–142. doi:10.1021/es00013a015

Carmo, A.M., L.S. Hundal, and M.L. Thompson. 2000. Sorption of hydrophobic organic compounds by soil materials: Application of unit equivalent Freundlich coefficients. Environ. Sci. Technol. 34:4363–4369. doi:10.1021/es000968v

Chen, Y., G. Sheng, X. Bi, Y. Feng, B. Mai, and J. Fu. 2005. Emission factors for carbonaceous particles and polycyclic aromatic hydrocarbons from residential coal combustion in China. Environ. Sci. Technol. 39:1861–1867. doi:10.1021/es0493650

Cornelissen, G., Ö. Gustafsson, T.D. Bucheli, M.T.O. Jonker, A.A. Koelmans, and P.C.M. van Noort. 2005. Extensive sorption of organic compounds to black carbon, coal, and kerogen in sediments and soils: Mechanisms and consequences for distribution, bioaccumulation, and biodegradation. Environ. Sci. Technol. 39:6881–6895. doi:10.1021/es050191b

Crittenden, J.C., S. Sanongraj, J.L. Bulloch, D.W. Hand, T.N. Rogers, T.F. Speth, and M. Ulmer. 1999. Correlation of aqueous-phase adsorption isotherms. Environ. Sci. Technol. 33:2926–2933. doi:10.1021/es981082i

De Jonge, H., and M.C. Mittelmeijer-Hazeleger. 1996. Adsorption of CO_2 and N_2 on soil organic matter: Nature of porosity, surface area, and diffusion mechanisms. Environ. Sci. Technol. 30:408–413. doi:10.1021/es950043t

Dubinin, M.M. 1960. The potential theory of adsorption of gases and vapors for adsorbents with energetically nonuniform surfaces. Chem. Rev. 60:235–241. doi:10.1021/cr60204a006

Gan, H., S.P. Nandi, and P.L. Walker, Jr. 1972. Nature of the porosity in American coals. Fuel 51:272–277. doi:10.1016/0016-2361(72)90003-8

Gregg, S.J., and K.S.W. Sing. 1982. Adsorption, surface area and porosity. 2nd ed. Academic Press, London.

Kärger, J., and D.M. Ruthven. 1992. Diffusion in Zeolites and other microporous solid. John Wiley & Sons, New York.

Kleineidam, S., C. Schuth, and P. Grathwohl. 2002. Solubility-normalized combined adsorption-partitioning sorption isotherms for organic pollutants. Environ. Sci. Technol. 36:4689–4697. doi:10.1021/es010293b

Kwon, S., and J.J. Pignatello. 2005. Effect of natural organic substances on the surface and adsorptive properties of environmental black carbon (char): Pseudo pore blockage by model lipid components and its implications for N_2–probed surface properties of natural sorbents. Environ. Sci. Technol. 39:7932–7939. doi:10.1021/es050976h

Larsen, J.W., P. Hall, and P.C. Wernett. 1995. Pore structure of the Argonne premium coals. Energy Fuels 9:324–330. doi:10.1021/ef00050a018

Lattao, C., X. Cao, Y. Li, J. Mao, K. Schmidt-Rohr, M.A. Chappell, L.F. Miller, A.L. dela Cruze, and J.J. Pignatello. 2012. Sorption selectivity in natural organic matter studied with nitroxyl paramagnetic relaxation probes. Environ. Sci. Technol. 46:12814–12822.

Li, J., and C.J. Werth. 2001. Evaluating competitive sorption mechanisms of volatile organic compounds in soils and sediments using polymers and zeolites. Environ. Sci. Technol. 35:568–574. doi:10.1021/es001366e

Luthy, R.D., G.R. Aiken, M.L. Brusseau, D.S. Cunningham, P.M. Gschwend, J.J. Pignatello, M. Reinhard, S.J. Traina, W.J. Weber, Jr., and J.C. Westall. 1997. Sequestration of hydrophobic organic contaminants by geosorbents. Environ. Sci. Technol. 31:3341–3347. doi:10.1021/es970512m

Mao, J.D., B. Xing, and K. Schmidt-Rohr. 2001. New structural information on a humic acid from two-dimensional ^{1}H-^{13}C correlation solid-state nuclear magnetic resonance. Environ. Sci. Technol. 35:1928–1934. doi:10.1021/es0014988

Milewska-Duda, J., J. Duda, A. Nodzenski, and J. Lakatos. 2000. Absorption and adsorption of methane and carbon dioxide in hard coal and active carbon. Langmuir 16:5458–5466. doi:10.1021/la991515a

Nam, K., and M. Alexander. 1998. Role of nanoporosity and hydrophobicity in sequestration and bioavailability: Tests with model solids. Environ. Sci. Technol. 32:71–74. doi:10.1021/es9705304

Ozdemir, E., B.I. Morsi, and K. Schroeder. 2005. CO_2 adsorption of Argonne premium coals. Fuel 83:1085–1094. doi:10.1016/j.fuel.2003.11.005

Pignatello, J.J. 2012. Dynamic interactions of natural organic matter and organic compounds. J. Soils Sediments 12:1241–1256. doi:10.1007/s11368-012-0490-4

Pignatello, J.J., and B. Xing. 1996. Mechanisms of slow sorption of organic chemicals to natural particles. Environ. Sci. Technol. 30:1–11. doi:10.1021/es940683g

Pignatello, J.J., S. Kwon, and Y. Lu. 2006. Effect of natural organic substances on the surface and adsorptive properties of environmental black carbon (char): Attenuation of surface activity by humic and fulvic acids. Environ. Sci. Technol. 40:7757–7763. doi:10.1021/es061307m

Ran, Y., W. Huang, P.S.C. Rao, D. Liu, G. Sheng, and J. Fu. 2002. The roles of condensed organic matter in the nonlinear sorption of hydrophobic organic contaminants by a peat and sediments. J. Environ. Qual. 31:1953–1962. doi:10.2134/jeq2002.1953

Ran, Y., B. Xiao, W. Huang, P. Peng, D. Liu, J. Fu, and G. Sheng. 2003. Kerogen in an aquifer material and its strong sorption for nonionic organic pollutants. J. Environ. Qual. 32:1701–1709. doi:10.2134/jeq2003.1701

Ran, Y., B. Xing, P.S.C. Rao, and J. Fu. 2004. Importance of adsorption (hole-filling) mechanism for hydrophobic organic contaminants on an aquifer kerogen isolate. Environ. Sci. Technol. 38:4340–4348. doi:10.1021/es035168+

Ran, Y., K. Sun, Y. Yang, B. Xing, and E.Y. Zeng. 2007. Strong sorption of phenanthrene by condensed organic matter in soils and sediments. Environ. Sci. Technol. 41:3952–3958. doi:10.1021/es062928i

Ravikovitch, P.I., B.W. Bogan, and A.V. Neimark. 2005. Nitrogen and carbon dioxide adsorption by soils. Environ. Sci. Technol. 39:4990–4995. doi:10.1021/es048307b

Reucroft, P.J., and A.R. Sethuraman. 1987. Effect of pressure on carbon dioxide induced coal swelling. Energy Fuels 1:72–75. doi:10.1021/ef00001a013

Schaumann, G.E. 2006a. Soil organic matter beyond molecular structure: Part II. Amorphous nature and physical aging. J. Plant Nutr. Soil Sci. 169:157–167. doi:10.1002/jpln.200521791

Schaumann, G.E. 2006b. Soil organic matter beyond molecular structure: Part I. Macromolecular and supramolecular characteristics. J. Plant Nutr. Soil Sci. 169:157–167. doi:10.1002/jpln.200521791

Schaumann, G.E., and E.J. LeBoeuf. 2005. Glass transitions in peat: Their relevance and the impact of water. Environ. Sci. Technol. 39:800–806. doi:10.1021/es0490931

Schaumann, G.E., E.J. LeBoeuf, R. DeLapp, and J. Hurrass. 2005. Thermomechanical analysis of air-dried whole soil samples. Thermochim. Acta 436:83–89. doi:10.1016/j.tca.2005.07.009

Steinberg, S.M., J.J. Pignatello, and B.L. Sawhney. 1987. Persistence of 1,2-dibromoethane in soils: Entrapment in intraparticle micropores. Environ. Sci. Technol. 21:1201–1208. doi:10.1021/es00165a007

Walker, P.L., Jr., and K.A. Kini. 1965. Measurement of the ultrafine surface area of coals. Fuel 44:453–459.

Walker, P.L., Jr., S.K. Verma, J. Rivera-Utrilla, and M.R. Khan. 1988. A direct measurement of expansion in coals and macerals induced by carbon dioxide and methanol. Fuel 67:719–726. doi:10.1016/0016-2361(88)90305-5

Weber, W.J., Jr., and W. Huang. 1996. A distributed reactivity model for sorption by soils and sediments: 4. Intraparticle heterogeneity and phase-distribution relationships under nonequilibrium conditions. Environ. Sci. Technol. 30:881–888. doi:10.1021/es950329y

Xing, B., and J.J. Pignatello. 1997. Dual-mode sorption of low-polarity compounds in glassy poly(vinyl chloride) and soil organic matter. Environ. Sci. Technol. 31:792–799. doi:10.1021/es960481f

Zhang, L., E.J. Leboeuf, and B. Xing. 2007. Thermal analytical investigation of biopolymers and humic- and carbonaceous-based soil and sediment organic matter. Environ. Sci. Technol. 41:4888–4894. doi:10.1021/es0631060

Zhou, L., S. Bai, W. Su, J. Yang, and Y. Zhou. 2003. Comparative study of the excess versus absolute adsorption of CO_2 on superactivated carbon for the near-critical region. Langmuir 19:2683–2690. doi:10.1021/la020682z

Zhu, X., I.L. Moudrakovski, and J.A. Ripmeester. 1997. ^{129}Xe NMR two-dimensional exchange spectroscopy of diffusion and transport in coal. Energy Fuels 11:245–246. doi:10.1021/ef960084q